

# DELINEATION OF MINERAL POTENTIAL ZONE USING GIS IN THE SOUTHERN PART OF LIBYA

Dr. Younes Ajal Abulghasem<sup>1</sup>, Dr. Ahmed Salem Saheel<sup>2</sup> and Dr. Tareq Hamed Mezughi<sup>3</sup>

**Abstract:** The powerful tools of Geographic Information System (GIS) and remote sensing (RS) have significantly contributed to the modern geological mapping and mineral exploration by enhancing, interpretation and integration of various geological datasets. Integration of remote sensing and airborne magnetic data with other geological data sets are the most promising and cost-effective method to add new structural and lithological aspects to the map of the geology in a diverse geological province as in the area of current research. This is due to the fact that all the geosciences information together with pre-processed remotely sensed data can be used as evidence to delineate possible areas for further study and more investigation (Chang-Jo & Fabbri 1993). The study area is a belt of Upper Devonian sedimentary formation including iron ore bearing layers, which extend over about 160km, in ENE-WSW direction, on the northern border of the Murzuq Basin. The study area is located in the western central part of Libya within the boundary's 27° South and 28° North Latitude and 12° to 16° East-longitude covering an area of nearly 40,000km<sup>2</sup>. This study examines the integration of aeromagnetic data with remote sensing to discover any probable extensions of iron ore deposits and any associated minerals in the area of study. The study involves analysis of magnetic data to delineate geological structures, faults and to extract important information about the locations of buried magnetic bearing rocks. Spatial data integration and analysis for the study area and predicting mineral potential were carried out on the available digital remote sensing data (Landsat ETM+). While searching for mineral potential areas, accurate and up-to-date geological maps are essential as it represents the most basic information for directing exploration activities. To this end, the existing geological map of the study area, which was published by Industrial Research Centre (IRC) in 1984, is too old to extract up-to-date information for mineral exploration. The main objective is to integrate these datasets to update the geological map and produce mineral potential map of the study area. In this research, the various datasets (aeromagnetic data, geological, remote sensing) were processed, integrated, and modeled using GIS techniques. The primary field study was conducted in the potential areas of the iron ore deposits. Few samples were collected from the area and subjected to XRF, XRD analyses. The produced Total Magnetic Intensity (TMI) map shows prominent NW-SE and N-NW trends. The Reduction to the Magnetic Pole (RTP) map is characterized by a dominant WNW-ESE trend in the study area. Total horizontal derivative of the pseudogravity map generally reflects fault or compositional changes which can be seen to describe structural trends. The central part of the study area can be divided into five zones where the eastern and northern zones show many short anomalies of NW-SE orientation and the southern zone shows E-W orientation, in the northern zone of the central part shows WNW-ESE orientation trends. Strong magnetic anomaly detected in the south of Idri Town can be interpreted as lenses of magnetite or magnetite-rich sandstone within the sedimentary rock sequence. The selective principal component analysis, band ratio, techniques allowed the discrimination of altered areas and the detection of iron and iron oxide bearing minerals. The most important finding in this study is discovering new potential areas covering about 1000km<sup>2</sup> of mineral deposits in the southeast and north-western parts of the area. These results increased the assumption of extending the iron ore belt under the sand dunes in the west and east parts of study area. The mineralogical analysis indicates that the iron ore type is goethite and hematite with percentage between 8 to 46 % Fe<sub>2</sub>O<sub>3</sub> associated with very important minerals such as pyrochlore (Na, Ca, U). Finally, new potential map mineral deposit was produced and classified into four zones which are low, moderate, high, and very high potential zone.

**Keywords:** Geographic Information System (GIS), Remote Sensing (RS), Wadi Ash Shati, Iron Bearing Layer, Landsat ETM+, Aeromagnetic Survey.

---

<sup>1</sup>Geologic Department, Faculty of Sciences, Alabel Alghrabi University.  
e-mail: younesajal17@gmail.com

<sup>2</sup>Exploration Department, Libyan Petroleum Institute (LPI), Tripoli-Libya.  
e-mail: a.saheel@lplibya.com

<sup>3</sup>Geography Department, Faculty of Arts, Tripoli University, Tripoli-Libya.  
e-mail: thmezughi@yahoo.com

## INTRODUCTION

Now days the interpretation of magnetic data has increased in the form of new models of the

causal body, after the development of computerized multiparameters inversion methods. Many of these permit interpreter interactions by the graphics display system for computer imposing geological allows sensitive that resulted in a significant increases in the use of the magnetic survey for mineral exploration. Over the past 40 years advances in measurement technology and digital recording of data, particularly on the extensive use of the air-magnetometer as a tool for geological mapping (Sharma, 1987). Aeromagnetic anomalies can be used to extract important information about the locations of buried faults and magnetic bearing rocks.

Geographic Information System (GIS) and Remote Sensing (RS) technology (RS) are very important tools in mineral exploration that large areas of land surface can be covered for detailed geological studies. Landsat ETM+ data provides a new digital geological mapping technique which can be used in this study to determine new potential areas for iron deposits. Integrating remote sensing data with geological and aeromagnetic data has the potential of delineating geological structures (e.g., fractures, faults) and ring system of the basement rocks, which possibly control the mineralization in the area.

XRD and XRF are very complementary methods to improve the analysis, the accuracy of phase identification and quantitative analysis. Those two methods increase the number of parameters measured, which means fewer assumptions required for analysis. This tour offers higher accuracy, not only results but also increases the range of measured samples. XRD is the most direct and accurate analysis of the present and the absolute number of mineral species in a sample to be determined. Ambiguous results can be achieved using XRD. In contrast, XRF provides very accurate information regarding the elemental composition of the sample. It has versatility in handling and conducting solids, accuracy and has excellent precision for the majority of the elements with its wide dynamic range from Oppm to 100% (Bonvin & Yellepeddi 2000).

### The Study Area

Wadi Ash Shati deposits are a belt of Upper Devonian sedimentary formation, including iron ore bearing layers, which extends over 160 km<sup>2</sup>, in ENE-WSW direction, on the northern border of the Murzuq Basin, in the province of Sabha (Fig. 1). The western and eastern ends of the iron ore bearing layers are covered by more recent formations, which completely cover the ore outcrops (Sterojexport



Fig. 1. location map of the study area

1977). The study area is situated in the province of Sabha, Libya, bounded by latitudes 27° and 28°N, and longitudes 12° and 16°E. The territory covers an area of nearly 40,000km<sup>2</sup>. The area of study lies to the south of the Gargaf Arch, an E-W trending anticline, built up of a Precambrian core and Cambrian to Devonian clastic sediments with Lower Carboniferous rocks at its southern fork, striking about 85° with 1-3° dip towards the south. Paleozoic formations containing iron-bearing oolitic layers are reported to occur in several areas beside the study area. The iron bearing deposit are mostly confined to the Middle and Upper Devonian Awaynat Wanin Formation. In the Shati Valley, the Upper Devonian formation consists of 140m of gray, tan and brown, fine to medium grained, well-rounded, and well-sorted cross bedded sandstone. It is interbedded with thin beds of quartzitic sandstone, varicoloured claystone and siltstone and contains several intraformational conglomerates.

**Aeromagnetic Survey:** The aeromagnetic data were provided by the Libyan Petroleum Institute (LPI), Tripoli, Libya, as grid data, with grid cell size of 1000m. The survey of the study area was carried out along a set of parallel flight lines at 2km spacing, while the flight height was 755m a.s.l. The aeromagnetic data were corrected and reduced to their final form. The magnetic intensity map was constructed with the aim of enhancing geological structures and for qualitative interpretation.

**Landsat ETM+ Image:** Three cloud-free Landsat ETM+ scenes of (186-41) acquired on October 7<sup>th</sup>, 2000, (187-41) acquired on March 9<sup>th</sup>, 2001 and

(188-41) acquired on March 9, 2001 provided by Industrial Research Centre (IRC), Tripoli, which covered the investigated area were used in this research. Thematic Mapper Plus (ETM+) instrument onboard this spacecraft is an eight-band multispectral scanning radiometer, capable of providing high-resolution imaging information of the earth's surface. The nominal ground sample resolution or "pixel" sizes are 15 meters in the panchromatic band, 30 meters in the 6 visible, near, and mid-infrared bands, and 60 meters in the thermal infrared band. Geological map of the study area NG33-1, NG33-2, G33.3 Scale 1:250,000 were published by Industrial Research Centre (IRC) Libya in 1984 used as a base map to extract the geological formations that were included in the study area and the previous structures map of lithology, tectonic and geologic setting.

**Field Data:** Three field visits in exploratory fieldwork are done in the study area to be familiarized with the general conditions of the area. The aims of fieldwork in this research are:

- 1 The information collected during fieldwork is the spatial distribution of rock units at the surface. This requires determining what rock units are exposed were on the surface, and tying that data to a geographic database, usually a topographic map or satellite image. This also requires determining the general composition of each rock type by visual identification. For most rock types, the minerals can be visually identified and other components using either the naked eye or a hand-held 10x pocket magnifier.
- 2 The second type of data collected is an actual sample of the different rock units encountered. Samples provide the ability to take the field units back into the laboratory, and to conduct more detailed examinations (XRD, XRF) on the composition and texture of the maps units seen in the field. Rock samples are collected as part of a field mapping exercise which invariably leads to a more complete understanding of the geology of a particular locality. Also, they needed to define the ore deposit types, the chemical composition and identify the percentage of iron.

## DATA PROCESSING

The methodologies applied in this study involved several steps. The literature review was the first step in deriving information about the general geology of the study area. This was followed by data preparation and pre-processing of aeromagnetic data remotely sensed images (Landsat ETM+).

## Total Magnetic Intensity (TMI)

The African Magnetic Map (AMMP) was a compilation of all available airborne, ground and marine magnetic data for the whole of Africa from (Getech et al, 2000). The used data, covering a variety of resolutions, vintages, and types, were merged into a unified 1km grid at a constant 1km elevation above terrain. International Geomagnetic Reference Field (IGRF) was removed from the original data with the use of computer program supplied by Geosoft package software. The total intensity map (Fig. 2) shows the magnetic field amplitude, which reaches 70nT, where it is relatively high comparing with its spatial distribution of the survey. The map shows an acute variation in the magnetic intensity, indicating variation in either lithology or basement topography. Sedimentary rocks are seen to be high magnetic and usually give only an insignificant contribution to the magnetic anomalies. The main sources of the magnetic anomalies are expected to depend on the basement setting and its magnetic features.

The total magnetic intensity (TMI) map of the south-eastern study area was obtained to delineate the subsurface structure (Fig. 2). The aeromagnetic anomalies range from -10 to 70nT and are characterized by both low and high frequencies of anomalies. The map reveals that the positive magnetic anomalies have a general E-W, N-S and NE-WS directions respectively. The configuration of positive anomalies could be attributed to relatively deep-seated low relief basement structure. The TMI anomalies could be strongly influenced by the regional tectonic. The negative magnetic anomalies have a generally N-S, E-W and ENE-WSW directions. The negative anomalies are related to shallow thick sediments. At low magnetic latitudes as is the case here, it is not very easy to correlate the observed anomaly maxima. The position of magnetic sources because in the TMI anomaly map, the maxima are not found vertically above magnetic sources, thus making it difficult to link the observed anomalies with the sources. To partially come to this, it is usually necessary the performer a standard phase shift operation known as reduction-to-pole on the observed magnetic field, the operator affects the phase as well as the amplitude.

## Reduction-to-the pole (RTP)

Reduction to the pole transformation of an anomaly in the fourier domain was used in Geosoft Package Software. RTP grids were easy to be interpreted because anomalies placed directly above the source of the magnetic field. The RTP transformation applied anomaly map was given in (Fig. 3) The inclination and declination angles of the ambient field were taken as 26.5°N and 14°E, respectively (38.44°N, -9.43°E). The RTP



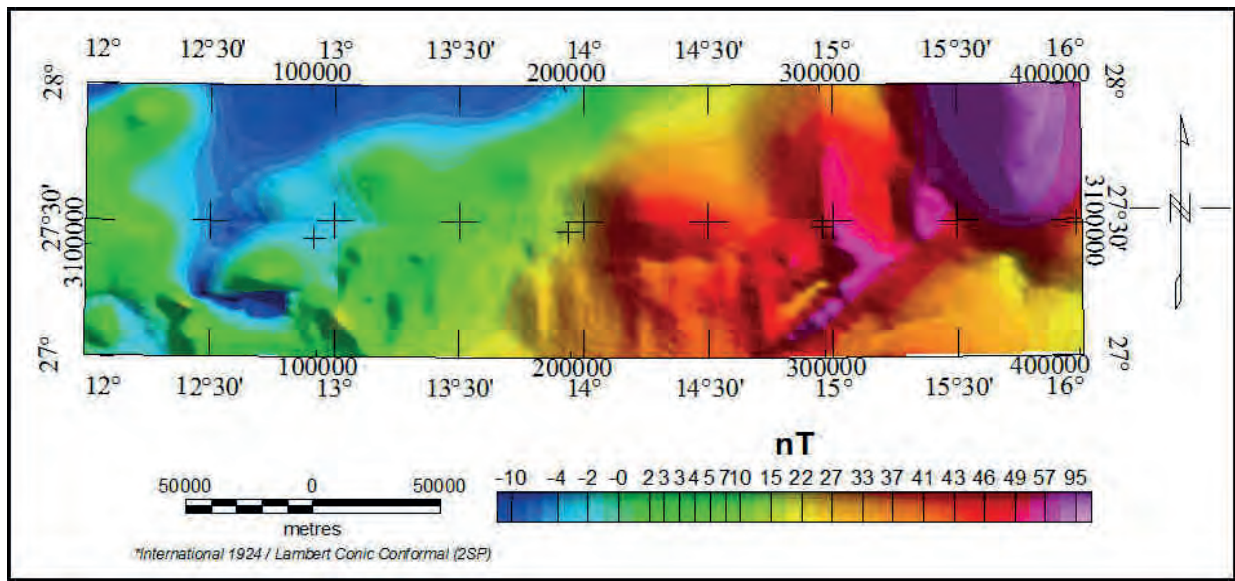


Fig. 2. Total Magnetic Intensity (TMI) map of the study area (Grid cell size 1000m).

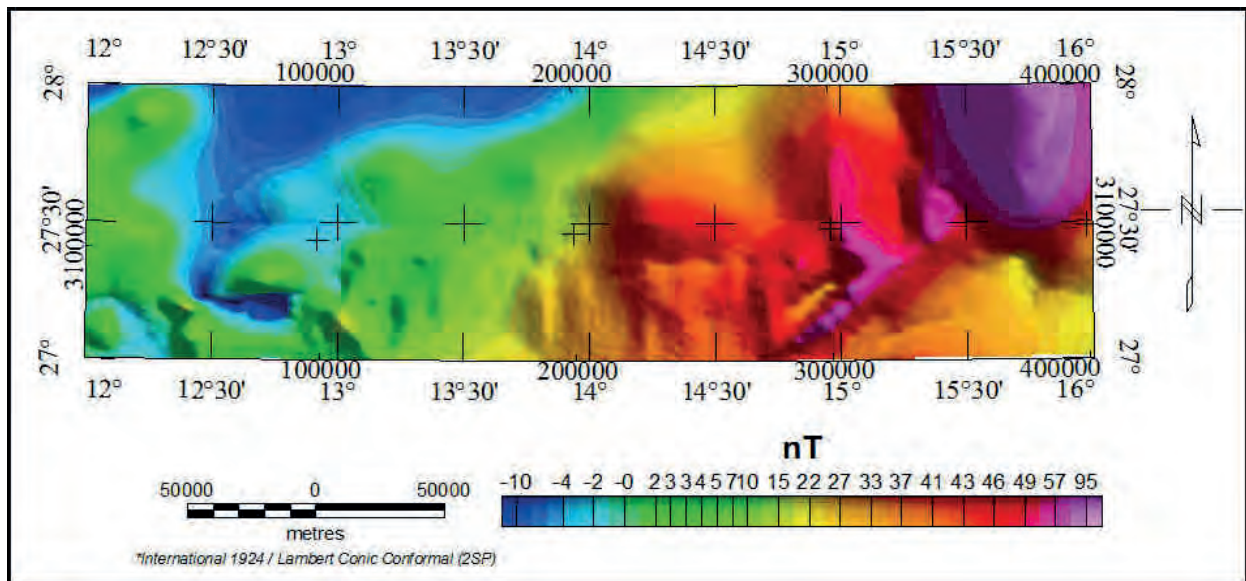


Fig. 3. Reduction to the pole map of the study area

aeromagnetic anomaly map (Figure 3) showed that both low and high frequency anomalies characterized the magnetic field in the study area. The elongated negative magnetic anomaly with values between  $-4$  to  $-10$  nT was observed over the locations of the western and eastern part of the study area. The extended negative magnetic anomaly was characterized by high frequency and high amplitude. Such magnetic anomaly is associated with thick sediment which was mainly recognized by high magnetic susceptibilities. This magnetic anomaly was bounded by steep magnetic gradients, which indicated the presence of two faults, trending in the NW-SE direction.

### The First Vertical Derivative (FVD)

Derivatives tend to sharpen the edges of anomalies and improve shallow features. The vertical derivative map is much more responsive to local influences than to broad or regional effects and therefore tends to give sharper picture than the map of total field intensity. Thus, the smaller anomalies are more readily apparent in area of strong regional disturbances. In fact, the FVD is used to delineate high frequency features more clearly where they are shadowed by large amplitude, low frequency anomalies. To emphasize the effect of the geological contact, critical for the structural framework of the area, the data processing involved accurate enhancement

of the short-wavelength and linear features. In that regard, the aeromagnetic data were first gridded with a grid-cell spacing of 1000m and were subjected to regional/residual separation to isolate short-wavelength signal which is more suitable for high-resolution mapping of shallow magnetic boundaries (Fig. 4). The regional/residual separation was made by subtraction of the upward-continued grid to 200m from the total magnetic intensity aeromagnetic grid. Upward continuation transformation attenuates high-frequency signal components and tends to emphasize deep, regional-scale magnetic anomalies. Subtraction of the low-frequency upward-continued data from the original grid produces a residual map that is enhanced in short-wavelength signal. The enhancement of magnetic anomalies associated with faults and other structural discontinuities were achieved by the application of FCD to the residual map in (Fig. 4 & Dobrin and Savit 1988; Telford *et al*, 1993). The reprocessed aeromagnetic data set is significantly enhanced in high frequency and is much better suited to detailed regional shallow mapping and analysis of basement magnetic boundaries.

### Pseudo-gravity

To locate and outline crustal magnetic sources, transformation techniques must be applied to the data as magnetic anomalies very rarely are centered above their source. The pseudo-gravity transform (Baranov, 1957) is applied to the magnetic data. By using the pseudo gravity transform, the apex of the magnetic anomalies is shifted over the source body and distortion due to the earth's magnetic field can easily be removed. A pseudo-gravity transformation

is useful in interpreting magnetic anomalies, not because a mass distribution actually corresponds to the magnetic distribution beneath the magnetic survey, but because gravity anomalies are in some ways more instructive and easier to interpret and quantify than magnetic anomalies (Blakely, 1995). The pseudo-gravity transform was applied to the total magnetic intensity grid using the FFT (Fast-Fourier-Transform) filter package available in Oasis Montaj by considering the density contrast of  $1\text{g/cm}^3$  and a magnetization of 0.5 Gauss. The pseudo-gravity field of the study area in magnetic anomaly for induced magnetization of the present-day field ( $I = 38.44^\circ$  and  $D = -9.19^\circ$ ) shows poor correlation with the observed total magnetic intensity anomaly (Fig. 5), suggesting that the causative body has a remnant magnetization. The contribution of the pseudogravity analysis permits us to better constrain the geodynamic of the study area.

### Total horizontal derivative technique

The Total Horizontal Derivative method (HD) was used for many years to locate density boundaries from gravity data (Cordell, 1979) and density and susceptibility boundaries from magnetic (as pseudogravity) data (Cordell and Grauch, 1985; Ma *et al*, 2006). These authors discussed a technique to estimate the location of abrupt lateral changes in magnetization or mass density of upper crust at rocks. The method is normally applied to mapped data rather than profiles. Maximum magnitudes of total horizontal gravity gradient normally occur above geological boundaries such as faults or steeply dipping lithological boundaries. Areas of

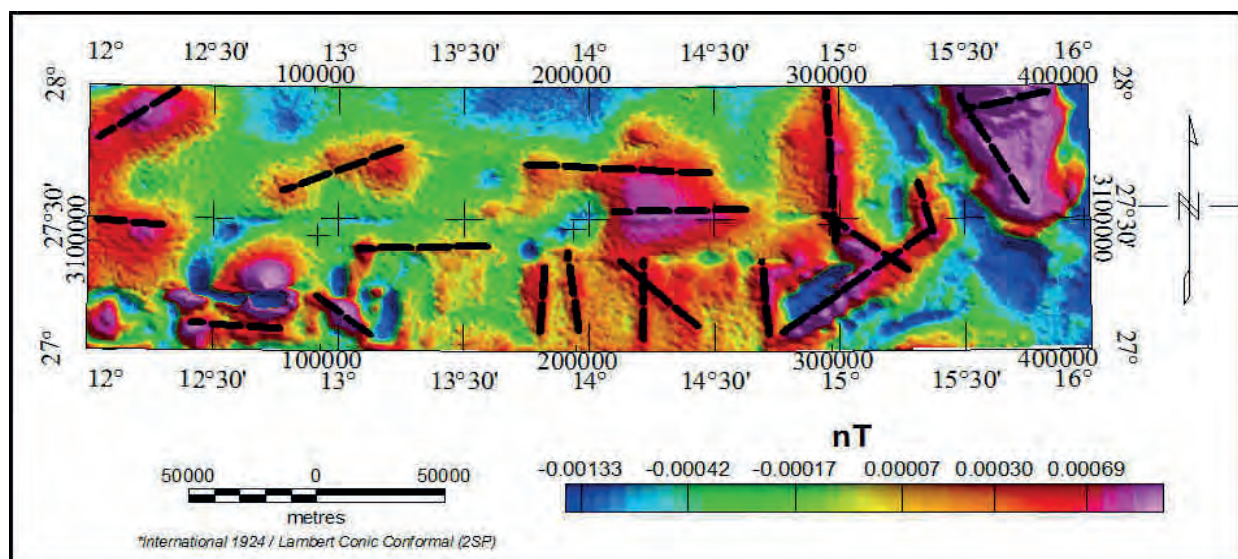


Fig. 4. First vertical derivative (FVD) of upward continuation 200m map of study area.



steep lateral gradients have higher scalar amplitude values of total horizontal gravity gradient (Blakely and Simpson, 1986). In applying this technique to a gridded dataset, the gridded pseudogravity for each grid point (x, y) is determined. Then the pseudogravity gradient function is calculated according to the following equation:

$$f = \sqrt{\left(\frac{\partial g}{\partial x}\right)^2 + \left(\frac{\partial g}{\partial y}\right)^2}$$

Where, f is “total horizontal gradient”,  $\left(\frac{\partial g}{\partial x}\right)$  is the x derivative and  $\left(\frac{\partial g}{\partial y}\right)$  is the y derivative. The technique is influenced by several factors such as dip of discontinuity, data spacing, reliability of data and density contrast. Shallow dipping faults

are shown in a position shifted in a downdip direction (Cordell and Grauch, 1985); Hansen and Pawlowski, 1989). In study area map of total horizontal gradient of pseudo-gravity grid data (Fig. 6), anomalies are observed throughout. The Map shows the present of total horizontal gradient anomalies especially in the eastern, western and central parts of the study area. In the eastern part, the strong anomaly is indicated trending in the NW-SE and NE-WS direction. About two anomalies are detected in the central part of the study area indicated NW-SE trending direction. One anomaly is observed in the western part of study area in the NW-SE direction.

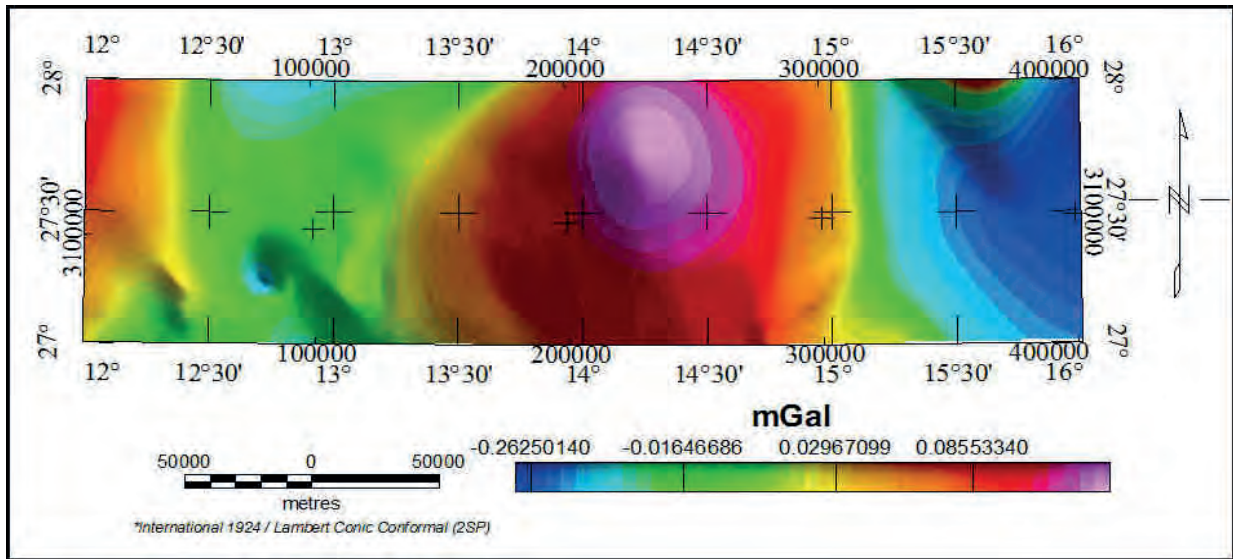


Fig. 5. Pseudogravity map of study area.

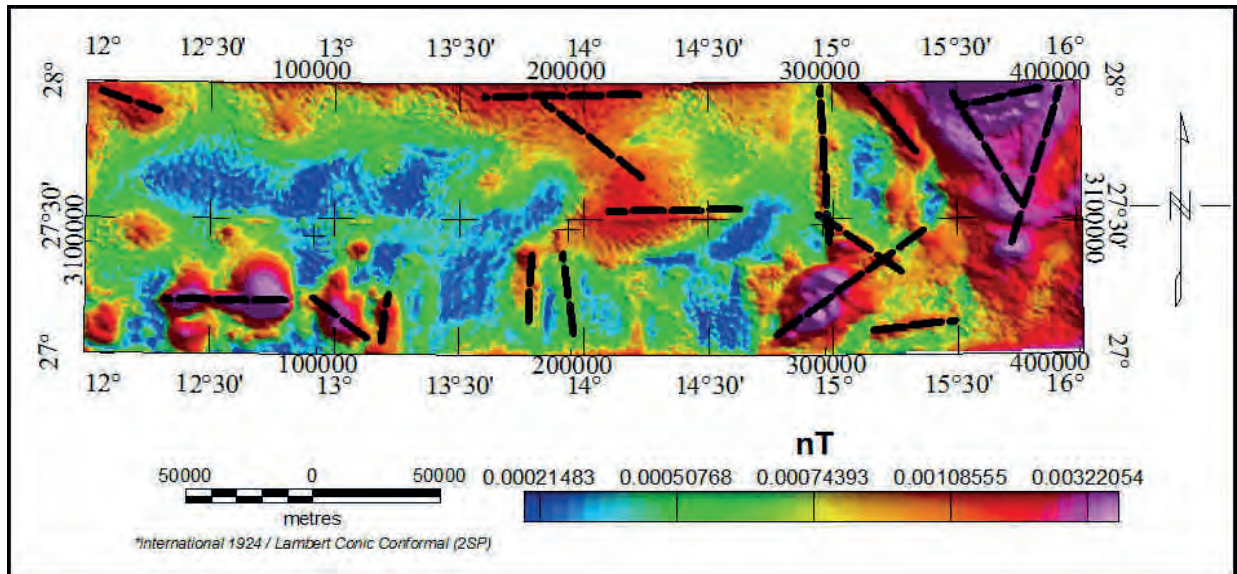


Fig. 6. Total horizontal gradient of Pseudogravity map of study area.

### Analytic Signal Method

The concept of analytic signal was provided by (Nabighian 1972; 1984) defined as a square root of the sum of the squares of the derivatives of total magnetic field in the x, y and z directions:

$$AS = \sqrt{\left(\frac{dT}{dx}\right)^2 + \left(\frac{dT}{dy}\right)^2} \sqrt{\left(\frac{dT}{dz}\right)^2}$$

The analytic signal is useful for locating the edges of magnetic source bodies, especially where remanence and low magnetic latitude complicate interpretation. Analytic signal picks up the highest amplitude anomalies (Fig. 7) and is independent of inclination of the geomagnetic field. The analytic signal signature of the study area was calculated in the frequency domain using the Fast Fourier Transform technique (Geosoft). The most of trending showing from analytic signal in the eastern part of study area direction NW-SE and NE-SW.

### Low-Pass and High-Pass Filtering

Filtering magnetic data is an essential process prior to analysis and interpretation. The purpose of the filter is to exceed the data set and make the presentation result in a way that it is easier to interpret the meaning of anomalies in relation to their geological sources. Therefore, the most effective way to filter data is by understanding the geological control and desired outcomes filtered. Multiple filtering techniques can be performed in the frequency domain. However, one of the most traditional filters used in the potential field, is the separation of long (deep) and short (shallow) wavelength anomalies. The success of this

technique depends on the correct choice of the cut-off wavelength of the filter design: The frequency bands corresponding to these linear segments which were used through the band pass filter technique to produce the low-pass and high-pass magnetic component maps. The regional (low-pass) magnetic anomaly maps, is characterized by large, homogenous and high-amplitude anomalies, which are caused by deep-seated causatives. The low-pass filter applied on reduced to the pole data to produce regional maps. The cut off wavelengths used were 10 000m, 15 000m, 20,000m, 25,000m, 30,000m, and 40,000m, the best result which presented the clear and smooth magnetic map found in wavelengths 30,000 (Fig. 8). The residual (high-pass) magnetic anomalies' maps were produced by subtracting total magnetic intensity (TMI) from the regional magnetic anomaly map, which was produced by (low pass) filter with cut off wavelengths 30,000m (Fig. 9). The (residual, regional, RTP, analytic signal and pseudo-gravity) maps were all subjected to horizontal derivative filter to delineate the lithological boundaries and faults' directions and to estimate the physical properties of the source structure causing the anomaly.

### Remote Sensing Data Processing

Pre-image processing such as radiometric and image enhancement were employed to clearly visualize the image. During the image processing, all images were geo-referenced into one projection system. Images were subseted to the bounding coordinates of the research area. Appropriate band combinations were chosen for and structural lithological interpretations.

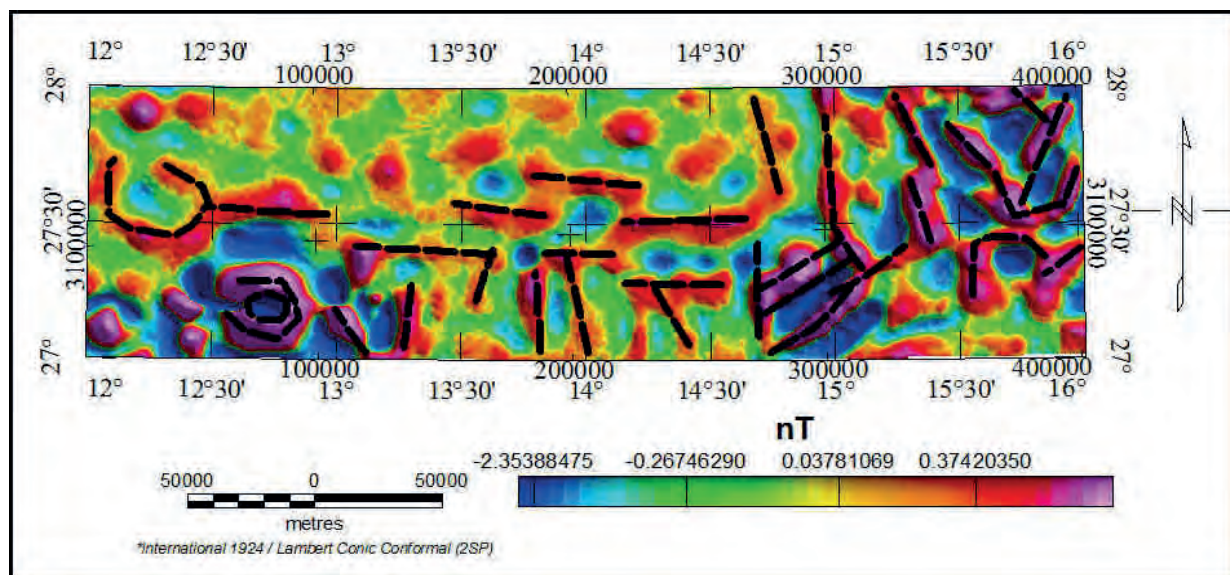


Fig. 7. Analytic signal of magnetic data of the study area.



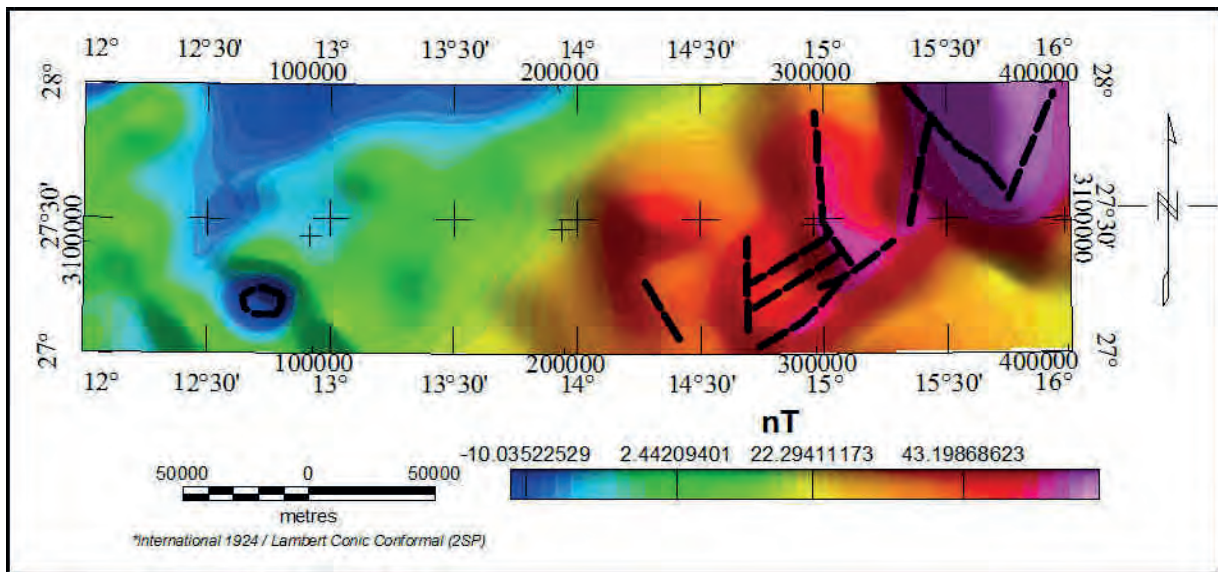


Fig. 8. Map showing low-pass filter for total magnetic Intensity data

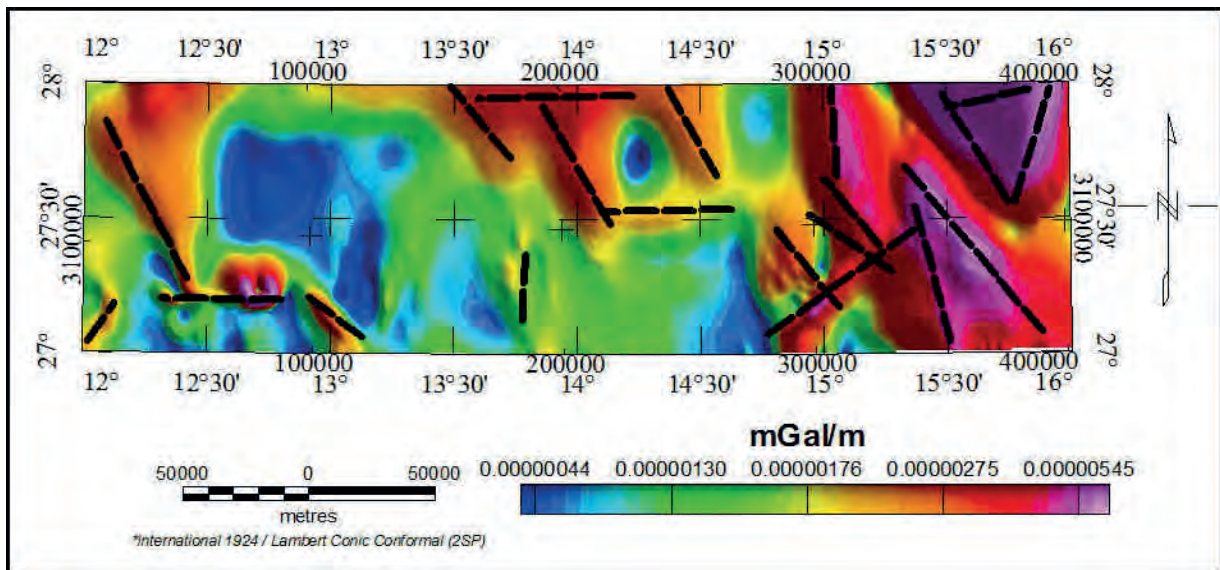


Fig. 9. Map showing high-pass filter for total magnetic Intensity data

**Supervised Classification Techniques:** Image classification is a very important method in the interpretation of remote-sensing data. The computer-assisted classification of an image automatically categorizes all pixels of an image into land cover classes (Poovalinga and Rajendram, 2009). The bands (7, 4, and 2) have been used in the image-supervised classification technique namely maximum likelihood classifier (MLC) to classify lithological units. Geologic maps for Idri and Wadi Ash Shati published in 1984 were used as reference ground data.

**Principal Component Analysis:** Principal component analysis (PCA) has been called one of the most valuable results from applied linear algebra. The “principal component analysis transformation,” is a multivariate statistical method used to compress multi spectral dataset into few PC images in which spectral difference between materials become apparent in PC image than individual bands (Gillespie *et al*, 1986; Sabins, 1987). Principal components are commonly calculated using the covariance matrix obtained from the input multi-spectral data whereby the corresponding Eigen matrices is also determined.



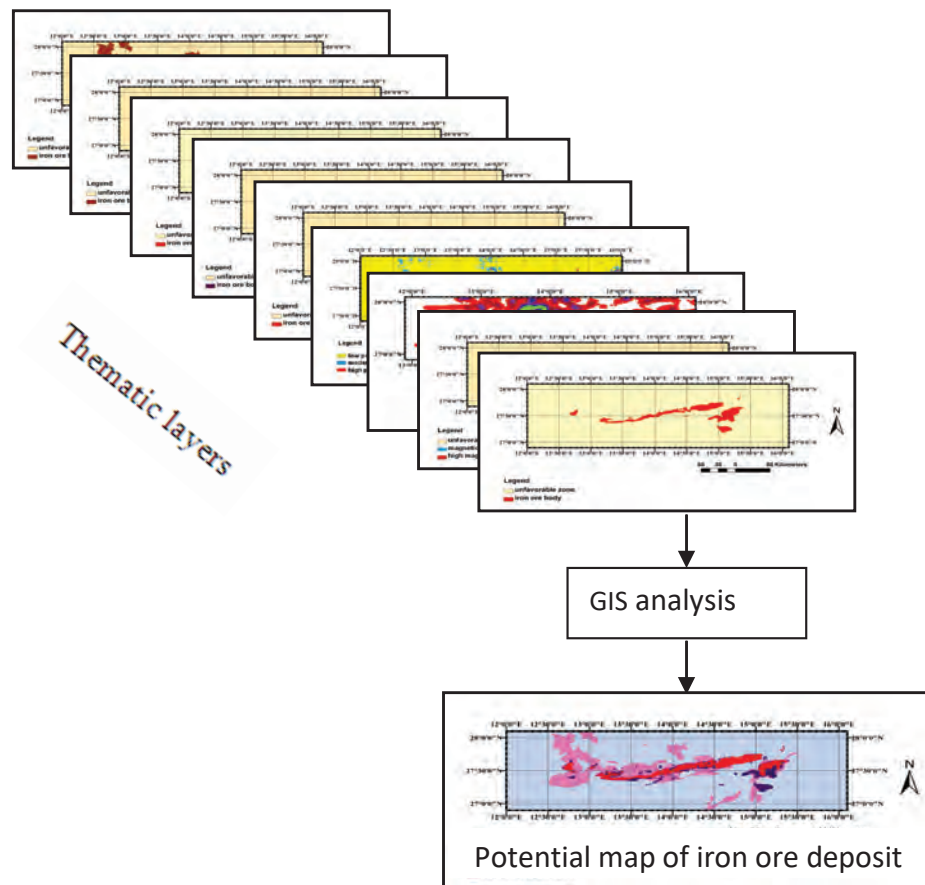


Fig. 10. GIS data analysis

**Band Ratio Technique:** In this study ratio image is mainly used for mineral alteration mapping, Landsat ETM+ bands selected for the band rationing for mineral alteration mapping is based on alteration minerals reflectance features. It is used here for lithologic investigation and mineral discrimination. The digital numbers were divided in a band by the DNs corresponding to a different tape for each pixel aspect ratio of the resulting value and draw the new values as an image.

**Lineament Extraction:** Different techniques of digital processing were applied to enhance and correct the acquired images as well as to choose the best band data for later analysis. From visual evaluation, band 7 of Landsat ETM+ image was selected for lineament analysis since it shows a better contrast and displays better visualization of geological features compared to the other band for each satellite. For lineament analyses spatial enhancement were performed using directional filters. Directional filters are quite useful for producing artificial effects, which may

reveal tectonically controlled linear features (Drury, 1987). Filtering technique was used to enhance the structural geological information (lineaments) for each selected band. Lineaments for directions (NS, NE-SW, E-W, NW-SE) are filtered separately, and then the tracings were overlapped to produce final lineaments map for each satellite. Sobel directional filter 3 by 3pixel kernels were applied to extract the lineaments in the area.

### GIS Analysis

**Thematic Map Preparation:** Getting an advantage of the power of GIS is to integrate various digital data set in a single unified database (Fig. 10), the maps which were extracted from, principal component analysis, band ratios, supervised classifications and geophysical data were digitized, analyzed and georeferenced with the same projection (geographic lat/long). The aim for this is to identify the areas of minerals occurrence and then combined in one map, which presents the potential areas of mineral deposit. After all data layers were extracted from remote-sensing data converted to raster format by digitizing

all those layers and save it in the same feature class under one geodatabase. The structure maps of the study area which were extracted from remote sensing and aeromagnetic results were integrated by using GIS system to produce one density structure map of the area. weighted overlay was used to combine all factor layer maps into new information to produce individual value for each pixel and a new map was produced (potential map). The weighting values used in the overlay operations were only performed on raster maps, and weighting value was given based on the influence of every subclass. The heuristic value for each factor and classification were given between 1 to 10, where value of 1 indicates that the influence or result towards is very low, while value 10 is very high. appropriate areas for mineral deposit were determined through six thematic layers: PCA, band-ratio, supervised classification, magnetic anomaly map, structure density map. Weights are assigned based on several experts' knowledge and by comparing each of these thematic layers with the geological map of the study area which are used as reference to define most accurate layers for highest weight and based on the conformation from the field trip and mineralogical analysis (Table 1) presents the weights assigned to every unit.

Table 1. Presents the weights assigned to every unit

Factor	Classes	i (rate)	W (weight)%
PCA 1, 2 & 3	Class 1	2	9
	Class 2	9	
PCA 7, 5 & 4	Class 1	2	7
	Class 2	9	
Band-ratio (5/4)	Class 1	1	9
	Class 2	2	
	Class3	9	
Supervised classification	Class 1	2	8
	Class 2	8	
Magnetic anomaly	Class 1	2	8
	Class 2	8	
	Class 3	9	
Density lineament Map	Class 1	1	3
	Class 2	2	
	Class 3	3	
	Class 4	4	

#### **Calculation of the sum of weights:**

$$PM = (SC * W + B1 * W + B2 * W + HIS * W + PC1 * W + PC2 * W + Mg * W + D * W)$$

Where PM = the final potential map of Wadi Ash Shati iron ore deposit and

SC= supervised classification map

B1= Band ratio map of bands 5/7, 5/4, 3/1

B2= Band ratio map of bands 5/4

IHS= Intensity-Hue-Saturation map

PC1= Principal Component map 7, 5 and 4

PC1= Principal Component map 1, 2 and 3

Mg= magnetic anomaly map

D= lineament density map

W= weight of each class

## **RESULTS AND DISCUSSION**

### **Magnetic Data**

The main results obtained in this study bring new elements allowing improvement of our knowledge on the geological structure of the study area spatial analysis, helped detect morphological differences in the lineament patterns. The eastern sector of the map shows a lineament toward WNW-ESE and ENE-WSW trend. The northern and western sectors of the map show of lineament toward NE-WSW. Accordingly, the terrain can be divided into tectonic sector. The comparison of the results with the geoscientific data (structural, lithological) confirms morphological difference. The tectonically subdivision into two tectonic corresponding to the Hercynian Croton in the eastern and western part of study area. Pan-African Croton in the southern east and helped identify the tectonic boundary separating them at depth assigned to the major normal faults in the centre. This geophysical study suggests that the structures of crust modeled are situated on the flank of the major faults in the basements it is a product of an active continental collision. This collision has provoked considerable over thrusting of the Pan-African Rift. The use of high-resolution magnetic data coupled with filter processing has increased the geologic information about the study area. Detailed magnetic interpretation can assist significantly in mapping the geology of the region.

### **Remote Sensing Data**

**Supervised Classification Technique:** The results of image classification show that the iron ore body (appears in red colour on the map) extends



towards the west and northwest of the known iron ore deposit (Wadi Ash Shati) and new areas of iron ore detected by supervised classification that these areas carrying the same DN value with the existing iron ore body. The results of supervised classification shown in (Fig. 11).

**Principal Component Analysis:** The PCA images were prepared using three visible (VIS) and three infrared bands of available sub-set of Landsat ETM+ mosaic. The first three PC images contain 98.33% of the information of the six Landsat-ETM+ bands. PC1, PC2, and PC3 display fair lithologic contrast and the rest of the PC (PC4 to PC7) appear to be less informative in terms of lithologic discrimination but the iron ore body still appears very clear. RGB composite of PC1, PC2 and PC3 have better colour contrast. It allowed best lithologic discrimination and the iron ore belt appears very clear in yellow colour on the map (Fig. 11). Landsat ETM+ image can be widely used to generate exploration targets in study area using the wavelengths characterized by iron absorption.

**Band ratio:** This technique is used to enhance contrasts between selected features and suppresses illumination differences between spectral features attributable to surface, look angle, and topographic effects. In a band ratio image, the black-and-white extremes represent areas with the greatest differences in the spectral reflectance of the two bands. Ratio image was produced using bands (5, 4), band ratio 5/4 has been computed to enhance possible ferrous oxides. The combination of ratio image 5/4 appears with black-and-white colour whereas, ferrous oxides appear with white colour and the rest of land cover appears with black thus this method very effective at detecting the ferrous oxides as shown in (Fig. 12).

**Lineament extraction:** The lineaments direction is parallel with the major faults reported by previous researchers. It seems that there is a relationship between the length of the lineaments and the orientation in the area, which means the length of the lineaments, plays the important role of certain orientations. The sun azimuth effect was clearly evidence of the appearing of lineaments in the EW & ENE-WSW directions (Figs. 13 & 14). Lineament density and intersection density of lineaments are also useful for characterizing the spatial patterns of lineaments (Figs. 15 & 16).

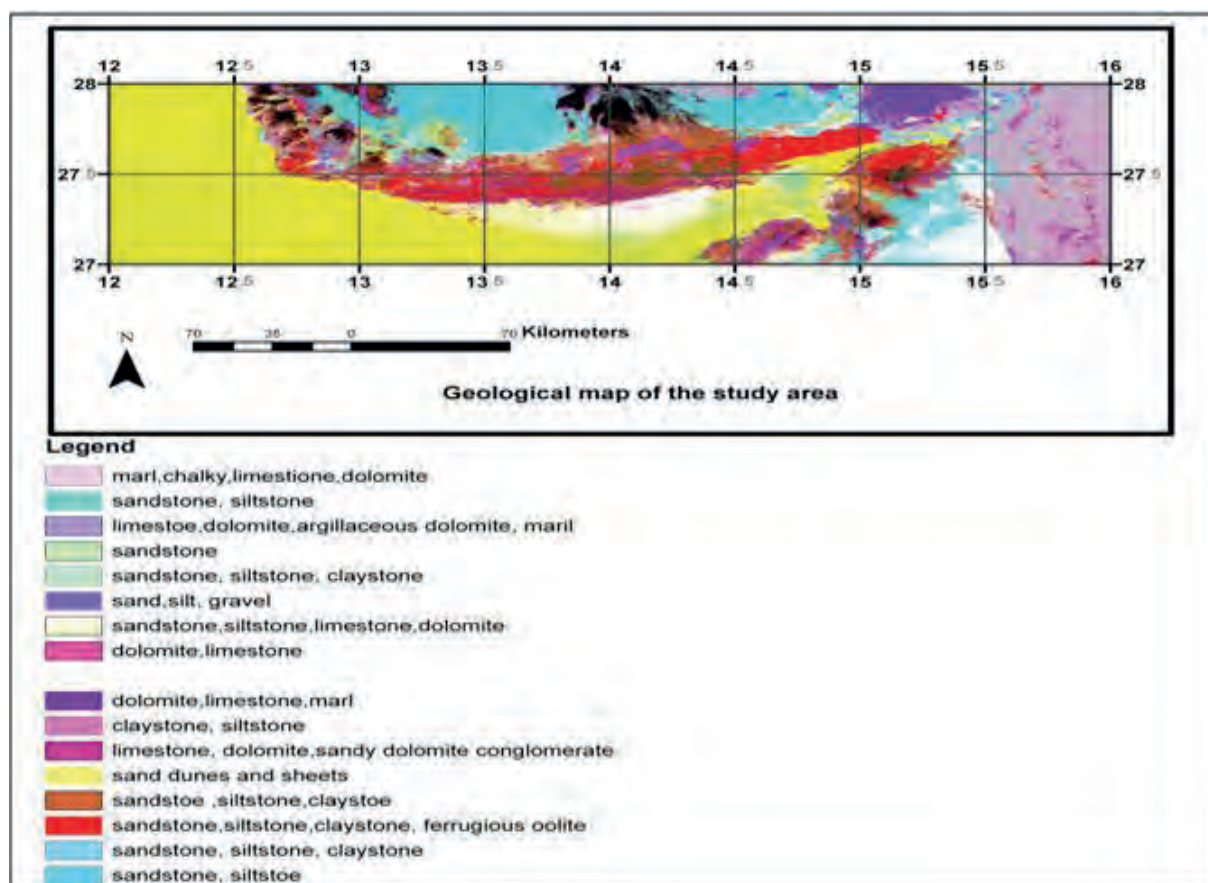
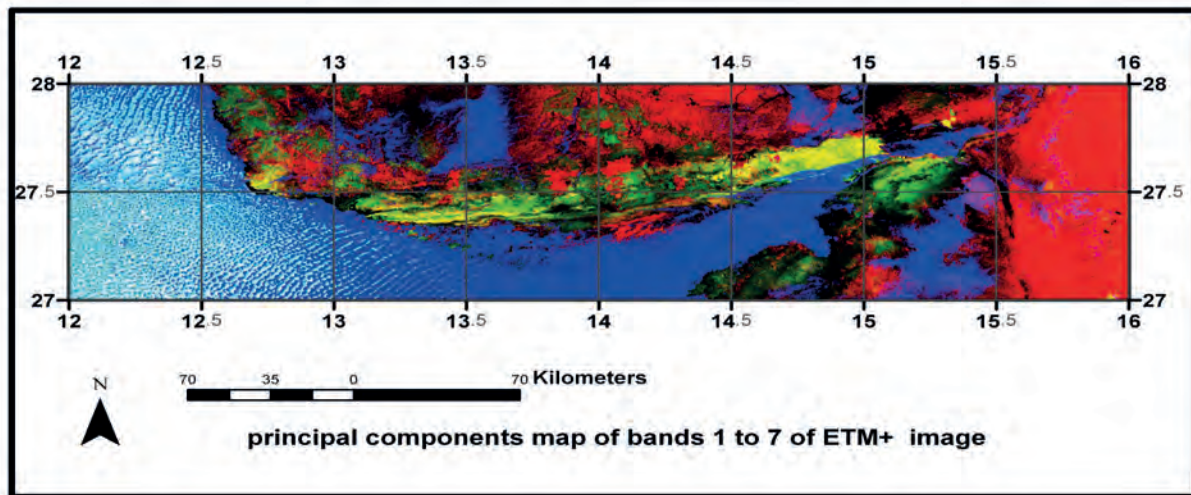


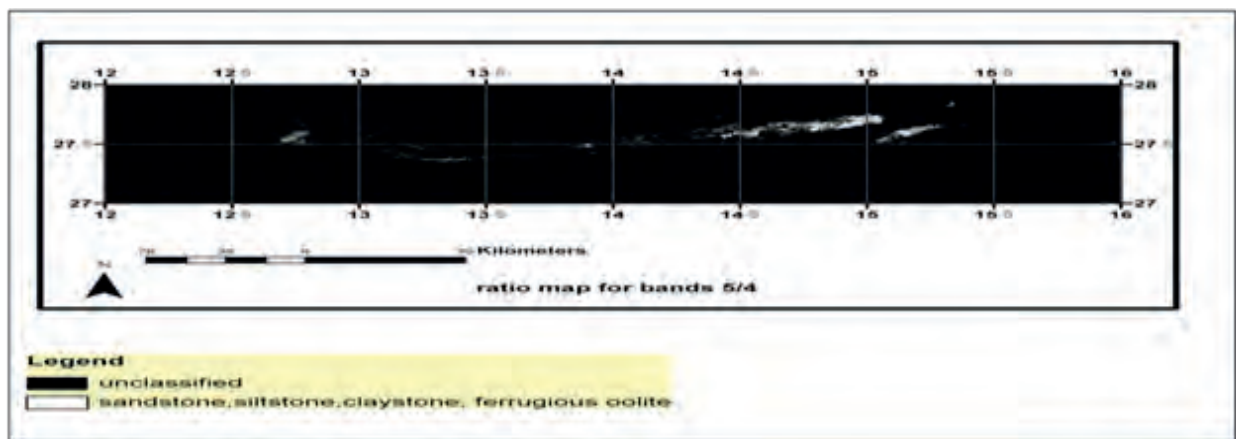
Fig. 11. Supervised classification map of the study area



#### Legend

- unclassified
- unclassified
- sand dunes and sheets
- sandstone, siltstone, claystone, ferrugious oolite

Fig. 12. Principal Analysis Component map of the study area



#### Legend

- unclassified
- sandstone, siltstone, claystone, ferrugious oolite

Fig. 13. band ratio map of the study area

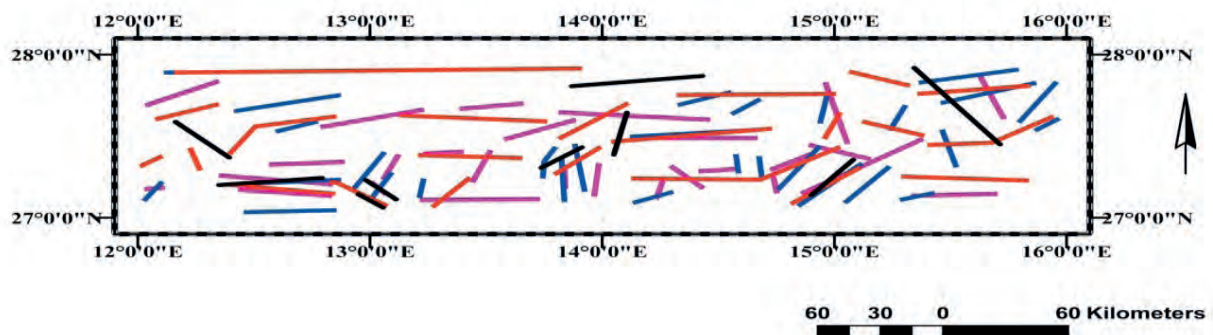


Fig. 14. New tectonic map of the study area showing tectonic elements derived from aeromagnetic data



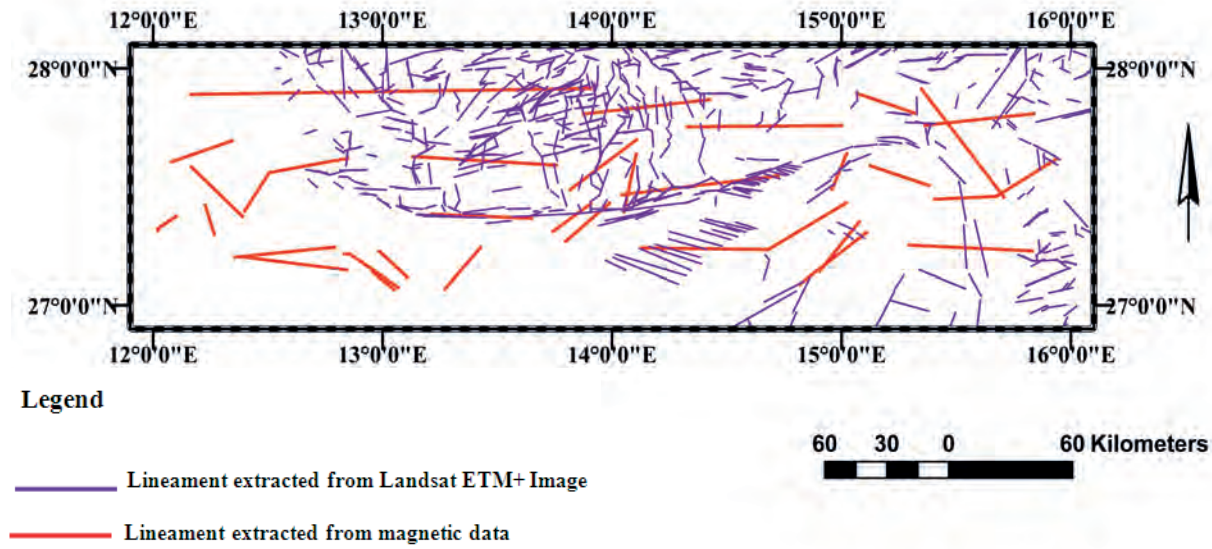


Fig. 15. Lineament map of the study area

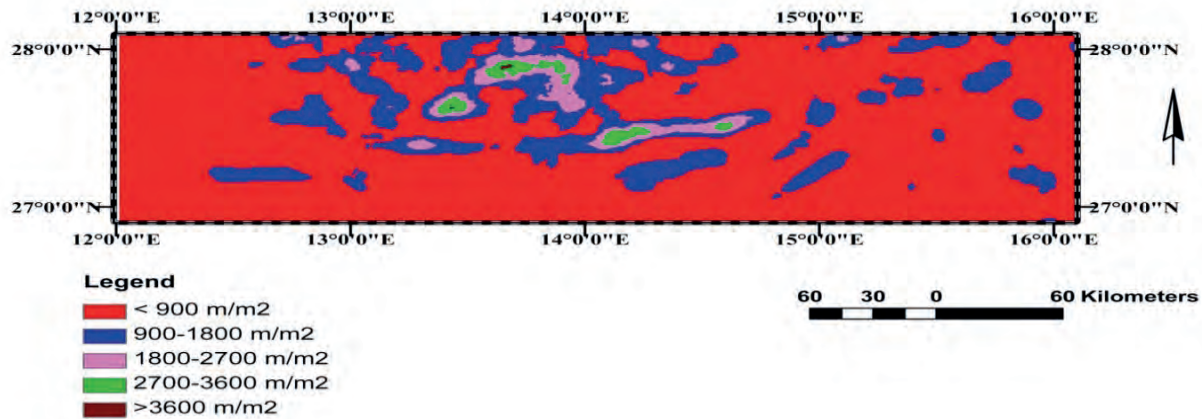


Fig. 16. Lineament density map of the study area

**Potential Map:** The delineation of iron ore deposit potential zones through the integration of different thematic layers obtained from remote sensing, aeromagnetic data interpretation and other secondary data have found to be effective techniques for analyzing the information content of each layer in GIS environment. The analysis would give meaningful results without the need of conducting fieldwork, which are time, effort and cost consuming activities. This technique would give broad ideas about the iron ore potentiality of the areas and then minimize the areas where iron ore deposit can be found and reduce the exploration activities to be carried out for subsurface study through geophysics

and drilling tests. The outcome of the application of remote sensing, aeromagnetic data and GIS on Wadi Ash Shatti area showed reasonable results where there was high potentiality on the areas of Wadi Ash Shatti valley and Idri Town. The Wadi Ash Shatti iron ore is one of the most important of mineral's deposit in Libya. Iron ore potential map generated through this process will help planners and decision makers for devising and feasible mining development plans. However, more field work still needs to be carried out to estimate the depth of the iron body and to estimate the volume of the lenses of the iron ore in the area. The new potential map was further classified into four zones which were low, moderate,

high and very high potential as shown in (Table 2). The moderate, high, and very high-potential zones in classified map were confirmed with evidence of geochemical analysis through the collected samples from the field (Fig. 17). The magnetic anomaly identified more potential zones within the boundaries of magnetic anomaly and new structure in the study area. This was deduced from the interpretation of the magnetic data, whereas the low potential zone still needs more study in terms of field visit and collecting samples for geochemical analysis and mineralogical investigation. However, the estimation of the exact amount of the iron ore is still not accurate and more iron ore is expected to be found in the potential area. Therefore, more boreholes are suggested to be drilled and more samples have to be collected and analysed especially from the classes of high and moderate in the new potential map. Figure (18) and Table (2) showing the area by km. sq. for each zone in the potential area.

## CONCLUSIONS

In this research, the various datasets available for the study area (remote sensing and aeromagnetic data) were processed, integrated, and modeled using Geographic Information System (GIS). The objective of this research was to integrate the available geological datasets to update the geological map and to produce an iron potential map in the study area. The magnetic survey data analyzed

using the most advanced and suitable techniques. This technique includes pseudo gravity, reduction to the pole filter, low-pass/high-pass filtering, and total horizontal derivative. The magnetic anomalies produced by deep geologic sources were separated from anomalies produced by shallow geologic effects using low-pass/high-pass filtering and depending on the anomalies' wavelength using matched band pass filtering. Tectonically, the magnetic methods were useful for detecting the geometry of the basement rocks, and the structures related to tectonic forces. The results indicate that the principal tectonic trend is oriented in the NE-SW direction (Fig. 14), which is found to be from the same direction of iron ore body in the study area. Magnetic data thus helped for extracting subsurface information to delineate host rocks and structural features which are responsible for mineral distribution in the study area. The magnetic intensity map showed clearly intrusive bodies, and a high magnetic anomaly observed in the southwest part of the study area probably caused by magnetic response of rocks is due to the presence of magnetic minerals such as magnetite, and hematite. This variation of susceptibility exists between different rock types. The basement is usually very vulnerable due to their high content of magnetite (iron), whereas sedimentary rocks have much lower susceptibilities. High-pass and low-pass filter techniques were used to decompose the magnetic

Table 2. Distribution of iron ore zones in the study area

Iron ore potential zone	Number of pixel	Area (Km2)
Very high zone	2480538398	2480
High zone	1124088208	1124
Moderate zone	1633129344	1633
Low zone	5540404361	5540

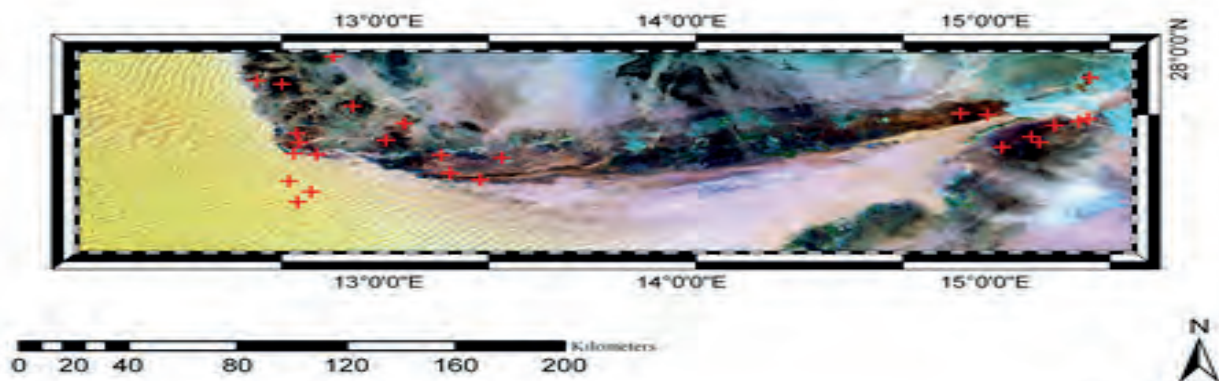


Fig. 17. Shows locations of collected samples from the study area



intensity map into the components related to shallow depths (residual anomalies) and those from deeper sources (regional anomalies). This study showed that integrating aeromagnetic with remote sensing data are an efficient tool for geological mapping. Different processing techniques were applied to the Landsat ETM+ and to discriminate and delineate the lithological units and regional lineaments. Moreover, remote sensing has proven a valuable aid in exploring mineral resources. New potential map of iron ore deposit in the study area was produced and

classified into four zones which were low, moderate, high and very high-potential zone (Fig. 18), based on the weight of each layer and the confirmation with evidence of geochemical analysis (XRD, XRF,) through the collected samples from the field (Table 3). The outcome of the application of remote sensing, aeromagnetic data and GIS in the study area showed reasonable results of high potentiality minerals (iron ore) associated with very important minerals (Pyrochlore) in Wadi Ash Shatti valley and Idri Town (Fig. 19).

Table 3. XRF results showing the percentage (%) composition of the samples

Element	Samples									
	S-NO-1	S-NO-2	S-NO-3	S-NO-4	S-NO-5	S-NO-6	S-NO-7	S-NO-8	S-NO-9	S-NO-10
SiO <sub>2</sub>	68.46	70.88	58.42	88.25	33.69	68.69	63.05	82.68	88.19	67.35
Fe <sub>2</sub> O <sub>3</sub>	29.37	22.06	32.67	8.51	45.69	29.09	33.6	10.37	9.13	27.11
CaO	0.72	5.28	7.00	0.97	9.4	0.18	0.1	3.34	0.61	1.42
P <sub>2</sub> O <sub>5</sub>	0.39	0.27	0.26	0.05	0.72	0.1	0.2	0.91	0.04	0.08
SO <sub>3</sub>	0.27	0.27	0.15	0.79	2.61	0.27	0.15	0.18	0.80	1.55
Al <sub>2</sub> O <sub>3</sub>	0.21	0.59	0.75	0.25	3.61	1.27	1.6	1.60	0.17	0.26
WO <sub>3</sub>	0.12	0.06	0.05	0.14	0.02	0.1	0.14	0.06	0.12	0.09
As <sub>2</sub> O <sub>3</sub>	0.09	0.04	0.00	0.00	0.00	0.00	0.00	29 PPM	0.00	0.00
MgO	0.07	0.23	0.18	0.07	1.26	0.04	0.05	0.40	0.05	1.25
Cl	0.05	0.03	0.01	0.02	0.42	0.02	0.02	0.02	0.01	0.10
Na <sub>2</sub> O	0.04	0.00	0.00	0.00	0.14	0.00	0.05	0.04	0.00	0.33
BaO	0.03	0.04	0.1	0.67	0.07	0.00	0.02	0.08	0.57	0.00
V <sub>2</sub> O <sub>5</sub>	0.03	0.03	0.02	0.00	0.07	0.02	0.01	0.02	0.00	0.00
MnO	0.03	0.05	0.16	0.02	0.77	0.01	0.07	0.06	0.02	0.14
TiO <sub>2</sub>	0.02	0.04	0.07	0.19	0.48	0.04	0.19	0.05	0.22	0.11
Gd <sub>2</sub> O <sub>3</sub>	0.02	0.02	0.02	0.00	0.00	0.02	0	0.00	0.00	0.02
Co <sub>2</sub>	0.02	0.00	0.02	0.01	0.03	0.00	0.1	0.00	0.00	0.00
K <sub>2</sub> O	0.01	0.04	0.02	0.02	0.00	0.00	0.65	0.00	0.01	0.06

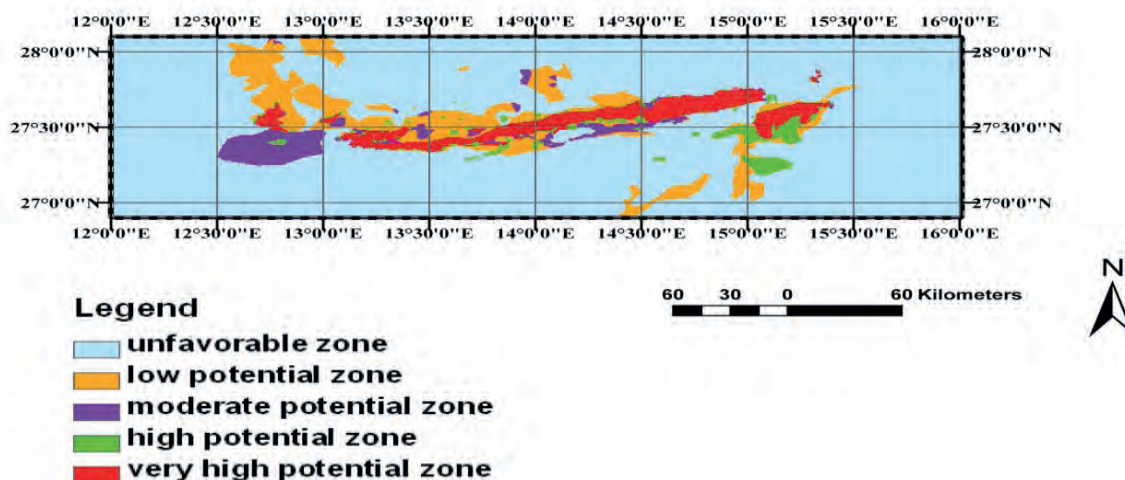


Fig. 18. Potential map of iron ore deposit in the study area include known iron ore deposit

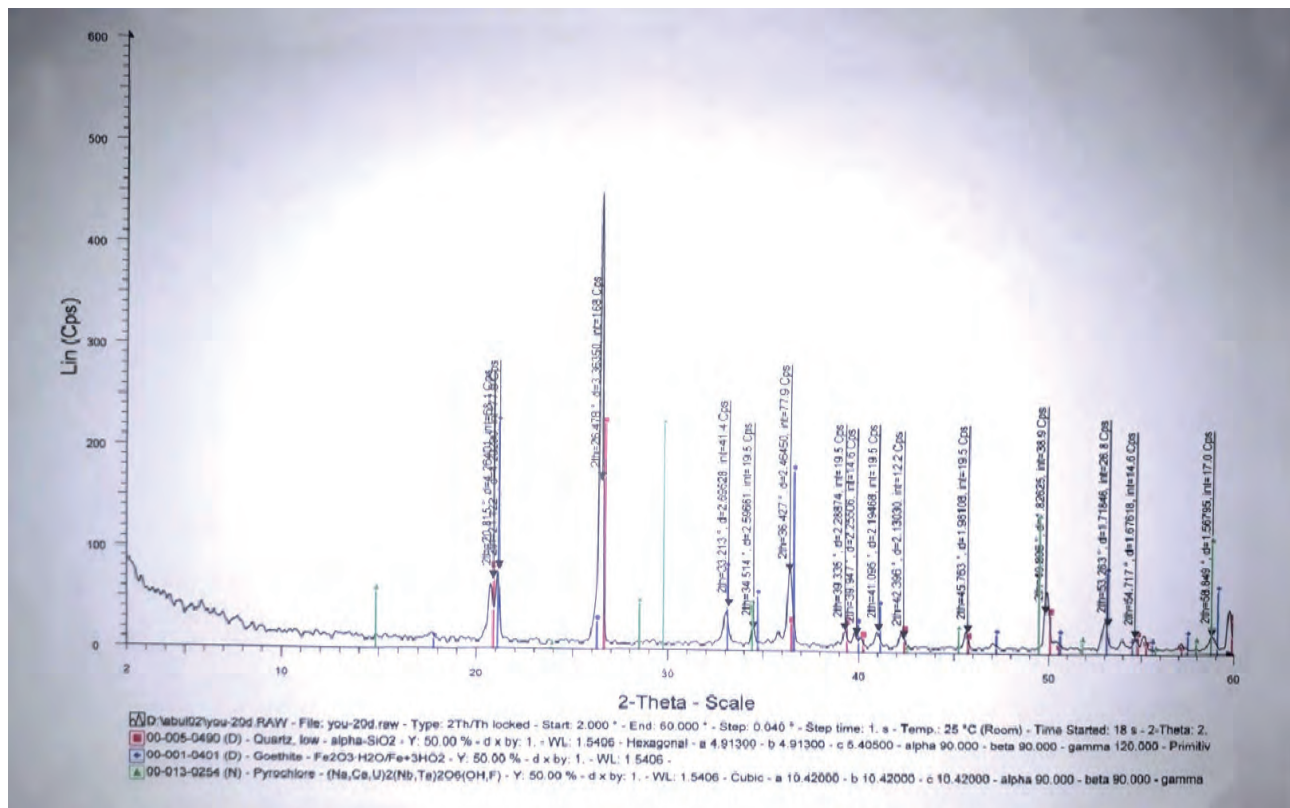


Fig. 19. Diffractograms the sample No (11) from study area shows the most important minerals (Pyrochlore) associated with Goethite and Quartz

## ACKNOWLEDGEMENTS

The authors wish to express their gratitude to National Oil Corporation of Libya (NOC) and LPI for providing magnetic data and the information's needed in this Paper.

## REFERENCES

- Baranov, V. (1957). A New Method for Interpretation of Aeromagnetic Maps: Pseudo-Gravimetric Anomalies, *Geophysics*, V. 22: 359-383.
- Blakely, R. J. (1995). *Potential Theory in Gravity and Magnetic Application*. Cambridge University Press London: 511p.
- Bonvin, D. & Yellepeddi, R. (2000). Applications and Perspectives of A New Innovative XRF-XRD Spectrometer In Industrial Process Control. Paper Read at Advances in X-ray Analysis: 126-136.
- Blakely, R. J. & Simpson, R. W. (1986). Locating Edges of Source Bodies from Magnetic and Gravity Anomalies. *Geophysics*, V.51(7):1494-1498.
- Chang-Jo, F. C., & Fabbri, A. G. (1993). Representation of Geoscience Information for Data Integration. *Nonrenewable Resources*:122-139.
- Cordell, L. (1979). Gravimetric Expression on Graben Faulting in Santa Fe Country and the Espanola Basin, New Mexico, Guidebo., 30th Filed Conf., Santa Fe Country, N.Mex. Geol. Soc.: 59-64.
- Cordell, L. and Grauch, V. J. S. (1985). Mapping Basement Magnetization Zones from Aeromagnetic Data in the San Juan Basin, New Mexico. The Utility of Regional Gravity and Magnetic Anomaly Maps, *Soc. Expl. Geoph.*: 181-197.
- Dobrin, M. B. and Savit, C. H. (1988). *Introduction to Geophysical Prospecting*. McGraw-Hill, New York: 867p.
- Drury, S. (1987). *Image Interpretation in Geology*, 3d ed. Allen and Unwin. V. 1: 48p.
- Geosoft, Reference Manual (2009). Software for Earth Sciences Geosoft INC., Toronto, Canada.
- Getech and Saad. Z J. (2000). Libya A Tectonic and Depth-to-Basement Study Using Well, Gravity and Magnetic Data, Unpublished report, No G0030.
- Gillespie, A. R.; Kahle, A. B. & Walker, R. E. (1986). Color Enhancement of Highly Correlated Images Decorrelation and HSI Contrast Stretches. In *Remote Sens. Envir.* New York, NY: 209-235.
- Hansen, R. O and Pawlowski R. S. (1989): Reduction to Pole at Low Latitudes by Weiner Filtering. *Geophysics*, V.54: 1607-1613.



- Ma, Z. J.; Gao, X. L. & Song, Z. F. (2006). Analysis and Tectonic Interpretation to the Horizontal-Gradient Map Calculated from Bouguer Gravity Data in the China Mainland. *Chinese Jour. Geophysics (Acta Geophysica Sinica)*, V.49(1): 106-114.
- Nabighian, M. N. (1972). The Analytic Signal of Two-Dimensional Magnetic Bodies With Polygonal Cross-Section: Its Properties and Use for Automated Anomaly Interpretation. *Geophysics*, V. 37: 507-517.
- Nabighian, M. N. (1984). Toward the Three Dimensional Automatic Interpretation of Potential Field Data Via Generalized Hilbert Transforms: Fundamental Relations. *Geophysics*, V.53: 957-966.
- Poovalinga, B. Rajendran, S. A. (2009). Visualizing Uncertainty-How Fuzzy Logic Approach Can Help to Explore Iron ore Deposits. *Indian Soc.Remote Sens.* V. 37: 1-8.
- Sterojexport. (1977). Clays Investigation of Wadi Ash Shat. Tripoli Industrial Research Center.
- Sabins, P. V. (1987). Magnetic Method Applied to Mineral Exploration, *Ore Geology Reviews*. In; P.V. Sharma (Ed.), V. 2(4): 323-357.
- Sharma, P. V. (1987). Magnetic Method Applied to Mineral Exploration, *Ore Geology Reviews*. In; P.V. Sharma (Ed.), V. 2(4): 323-357.
- Industrial Research Centre (1984). Geological Map of Libya: Sheet Sabha- NG 33-1,33-2, 33-3, With Explanatory Book.
- Telford, M. W.; Geldart, P. L. & Sheriff, E. R. (1993). *Applied Geophysics*, 2d Edition. Cambridge University Press: 769p.

## ABOUT THE AUTHORS



**Dr. Younes Ajal Abulghasem** qualification is as following:

PhD (Geology / Remote Sensing), University Kebangsaan Malaysia (UKM), 2014

MSc (Remote Sensing and GIS) University Putra Malaysia (UPM), 2005

MSc Information technology (IT) Golden State University, 2004.

B.Sc (Geology) Tripoli university , 1992.

Dr Younes is working with the Geologic Department, Faculty of Sciences. Aljabel Alghrabi University.

*e-mail: younesajal17@gmail.com*



**Tareq Hamed Mezughi** is a Lecturer at University of Tripoli, Department of Geography and GIS. Dr Tareq has got his B.Sc in the field of Geology in 1988 from Tripoli University , Libya. He did his M.Sc in Remote Sensing, Image Processing and Application at the University of Dundee, UK in 1997.

*e-mail: thmezughi@yahoo.com*



**Dr. Ahmed Salem Saheel** has got his B.SC. from the Faculty of Petroleum & Mining Engineering, Geophysics Department, Tripoli University, Libya. He finished MPhil at the Earth Science Department, Leeds University, UK in 1995. Dr Saheel got Ph.D. from the Faculty of Science and Technology, Universiti Kebangsaan Malaysia, Malaysia in 2014. He is working with the Libyan Petroleum Institute, Exploration Department, Tripoli, Libya.

*e-mail: a.saheel@lpilibya.com*